Comparison of WENO scheme and high-order WENO-gas-kinetic scheme for inviscid and viscous flow simulation

Jun Luo

Department of Mathematics

Hong Kong University of Science and Technology

Hong Kong, China

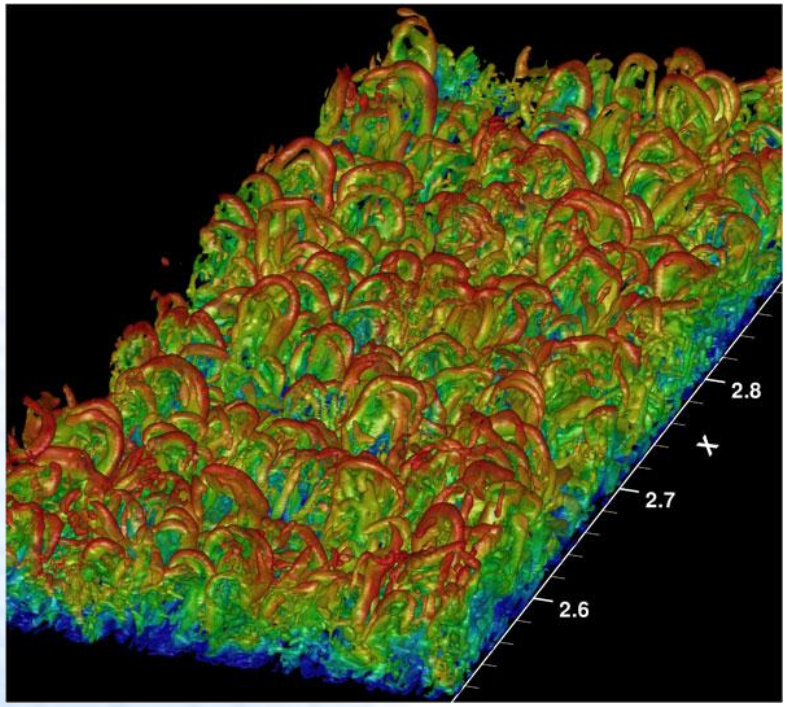
2.8
2.7
2.6

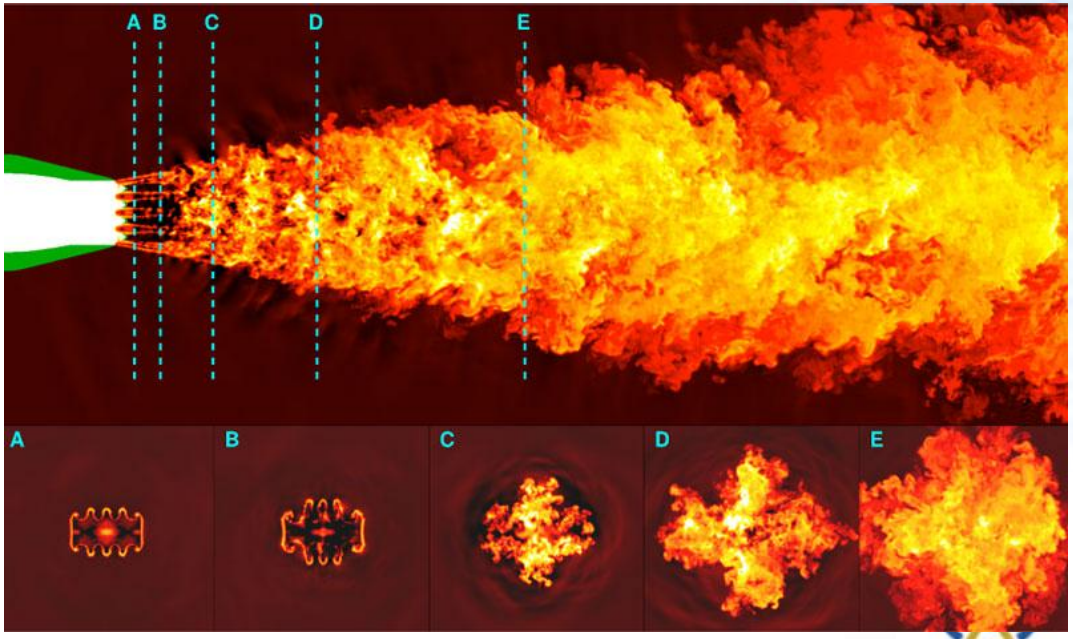
A
B
C
D
E
A
B
C
D
E

Contents

- PDE-based modeling
- A high-order WENO-gas-kinetic Navier-Stokes flow solver
- The WENO-Steger-Warming scheme
- Numerical results
- Conclusion

PDE-based modeling

Conservation Laws:

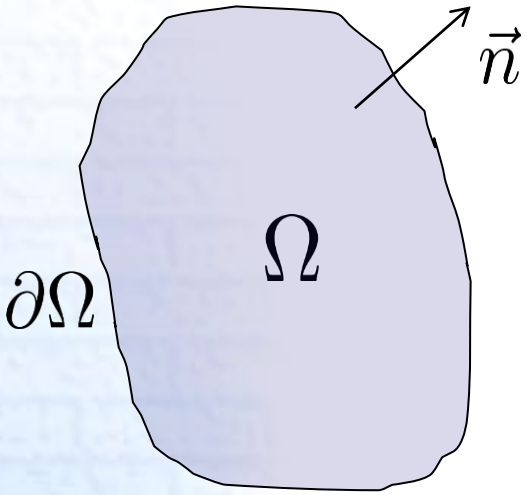

or

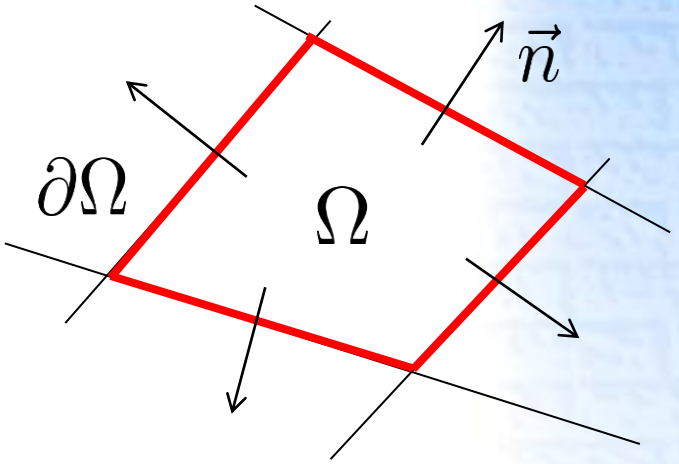

$$\int_{t^n}^{t^{n+1}} \iint_{\Omega} W(x,t)d\vec{x}dt = -\int_{t^n}^{t^{n+1}} \int_{\partial\Omega} F(\vec{x}(s),t)dsdt + \int_{t^n}^{t^{n+1}} \iint_{\Omega} S(\vec{x},t)d\vec{x}dt$$

$W(x,t)$: density of any conservative variable

F : flux along the outward normal direction $\vec{n}$ of $\partial\Omega$

s : the parameter used to define $\partial\Omega$

S : source term

t^n : the time at the nth time step

PDE-based modeling

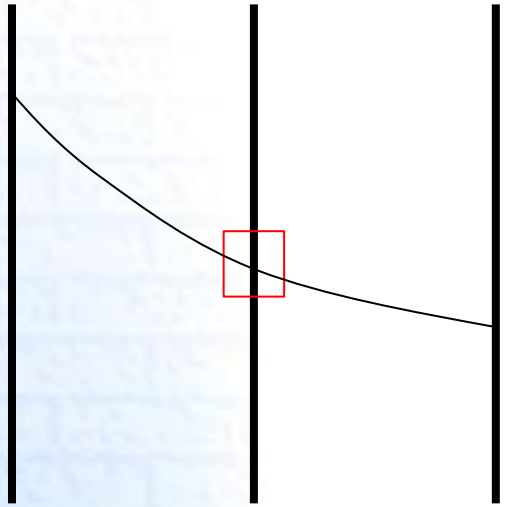

Continuous

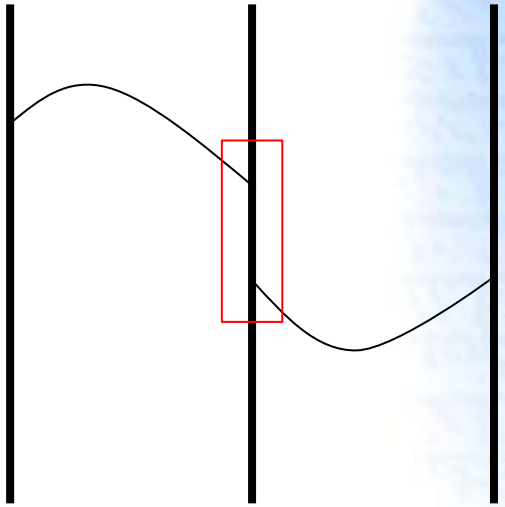

Discontinuous

The use of Euler equations in a highly non-equilibrium flow region is problematic.

Contents

- PDE-based modeling
- A high-order WENO-gas-kinetic Navier-Stokes flow solver
- The WENO-Steger-Warming scheme
- Numerical results
- Conclusion

A high-order NS solver

Bhatnagar-Gross-Kook (BGK) equation:

$$f_t + \vec{u} \cdot \nabla f = \frac{g - f}{\tau}$$

f : gas distribution function
$\vec{u}$: particle velocity
g : equilibrium distribution function approached by f
τ : particle collision time, $\tau = \mu / p$
μ : dynamic viscosity coefficient
p : pressure.

In 2-D case:

$$\vec{x} = (x, y),\ \vec{u} = (u, v)$$

A high-order NS solver

$W = (\rho, \rho U, \rho V, \rho E)^T$: mass, momentum and energy density

(U, V): macroscopic velocity of the fluid

$$W = \iiint \psi f \mathrm{d}u\mathrm{d}v\mathrm{d}\xi$$

$$\psi = (\psi_1, \psi_2, \psi_3, \psi_4)^T = (1, u, v, \frac{1}{2}(u^2 + v^2 + \xi^2))^T$$

$d\xi = d\xi_1 d\xi_2 ... d\xi_K$

K: number of degrees of internal freedom

$K = (4 - 2\gamma)/(\gamma - 1)$ in 2-D

γ: specific heat ratio

A high-order NS solver

The mass, momentum, and energy are conserved during particle collisions.

$$\iiint (g - f)\psi_\alpha \mathrm{d}u\mathrm{d}v\mathrm{d}\xi = 0, \qquad \alpha = 1, 2, 3, 4$$

g is a Maxwellian distribution function, i.e.,

$$g = \rho \left(\frac{\lambda}{\pi}\right)^{\frac{K+1}{2}} e^{\lambda((u-U)^2+(v-V)^2+\xi^2)}$$

$\lambda = m/(2kT)$

m: molecular mass

k: Boltzmann constant

T: temperature

A high-order NS solver

The NS distribution the Chapman-Enskog (CE) expansion of BGK equation:

$$f_{NS}(\vec{x},t,\vec{u},\xi) = g(\vec{x},t,\vec{u},\xi) - \tau[g_t(\vec{x},t,\vec{u},\xi) + \vec{u}\cdot\nabla g(\vec{x},t,\vec{u},\xi)]$$

The integral solution of BGK equation:

$$f(\vec{x},t,\vec{u},\xi) = \frac{1}{\tau}\int_0^t e^{-(t-t')/\tau} g(\vec{x'},t',\vec{u},\xi)dt' + e^{-t/\tau} f_0(\vec{x}-\vec{u}t,\vec{u},\xi)$$

$$\vec{x'} = \vec{x} - \vec{u}(t-t')$$

$f_0(\vec{x},\vec{u},\xi)$: initial distribution function.

A high-order NS solver

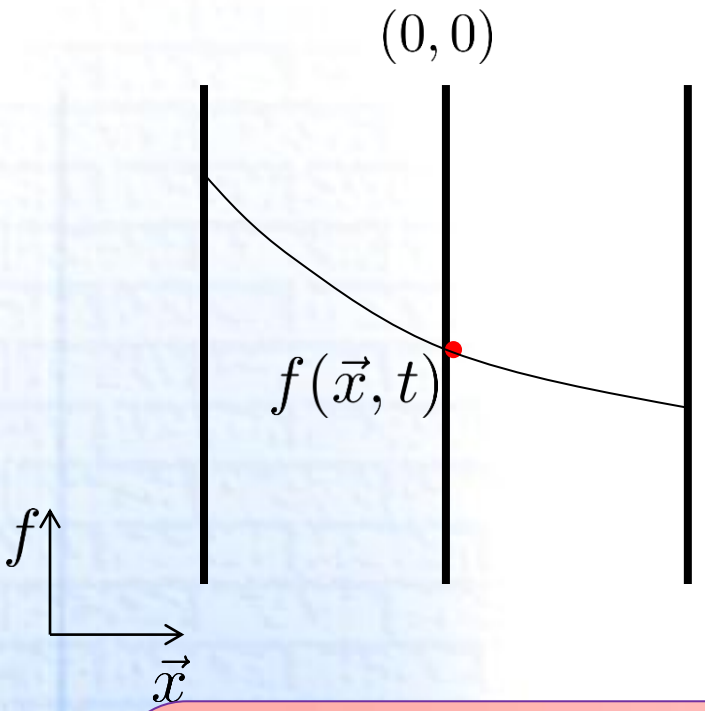

Continuous modeling:

Taylor expansion of the NS distribution function around $(0,0)$ gives the local continuous distribution function at the cell interface.

$$f(\vec{x},t) = f_{NS}(0,0,0) + \frac{\partial f_{NS}}{\partial x}\Big|_{(0,0,0)} x + \frac{\partial f_{NS}}{\partial y}\Big|_{(0,0,0)} y + \frac{\partial f_{NS}}{\partial t}\Big|_{(0,0,0)} t$$

$$+\frac{1}{2}\frac{\partial^2 f_{NS}}{\partial x^2}\Big|_{(0,0,0)} x^2 + \frac{1}{2}\frac{\partial^2 f_{NS}}{\partial y^2}\Big|_{(0,0,0)} y^2 + \frac{\partial^2 f_{NS}}{\partial x \partial y}\Big|_{(0,0,0)} xy$$

$$+\frac{1}{2}\frac{\partial^2 f_{NS}}{\partial t^2}\Big|_{(0,0,0)} t^2 + \frac{\partial^2 f_{NS}}{\partial x \partial t}\Big|_{(0,0,0)} xt + \frac{\partial^2 f_{NS}}{\partial y \partial t}\Big|_{(0,0,0)} yt.$$

A high-order NS solver

Initial reconstruction:

$$W(x,y) = W(0,0) + \frac{\partial W}{\partial x}\Big|_{(0,0)} x + \frac{\partial W}{\partial y}\Big|_{(0,0)} y + \frac{1}{2}\frac{\partial^2 W}{\partial x^2}\Big|_{(0,0)} x^2 + \frac{1}{2}\frac{\partial^2 W}{\partial y^2}\Big|_{(0,0)} y^2 + \frac{\partial^2 W}{\partial x \partial y}\Big|_{(0,0)} xy$$

$$\iiint g(0,0,0)\psi \mathrm{d}u\mathrm{d}v\mathrm{d}\xi = W(0,0,0)$$

$$\iiint g_x(0,0,0)\psi \mathrm{d}u\mathrm{d}v\mathrm{d}\xi = \frac{\partial W}{\partial x}\Big|_{(0,0)}$$

$$\iiint g_y(0,0,0)\psi \mathrm{d}u\mathrm{d}v\mathrm{d}\xi = \frac{\partial^2 W}{\partial y}\Big|_{(0,0)}$$

$$\iiint g_{xx}(0,0,0)\psi \mathrm{d}u\mathrm{d}v\mathrm{d}\xi = \frac{\partial^2 W}{\partial x^2}\Big|_{(0,0)}$$

$$\cdots$$

$$f_{NS}(\vec{x},t) = g(\vec{x},t) - \tau[g_t(\vec{x},t) + \vec{u}\cdot\nabla g(\vec{x},t)]$$

$$\iiint [g_t(\vec{x},t) + \vec{u}\cdot\nabla g(\vec{x},t)]\psi \mathrm{d}u\mathrm{d}v\mathrm{d}\xi = 0$$

A high-order NS solver

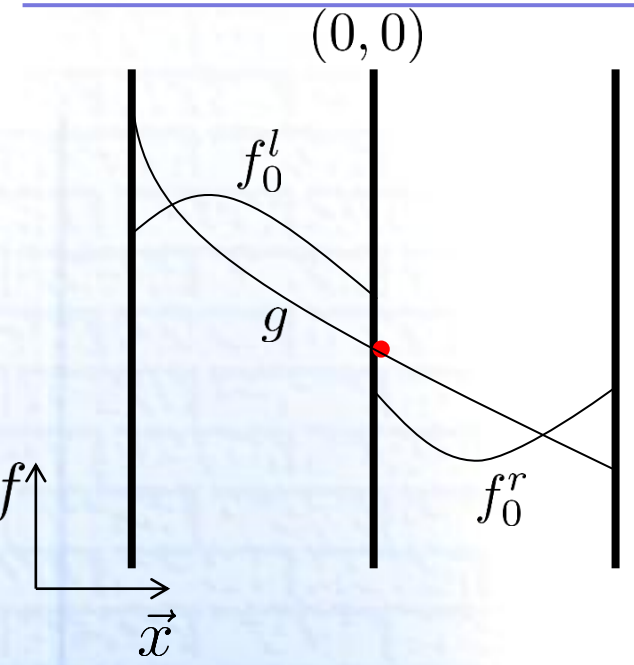

Discontinuous modeling:

Get the distribution function at the cell interface through the integral solution.

$$f(\vec{x},t,\vec{u},\xi)=\frac{1}{\tau}\int_0^t e^{-(t-t')/\tau}g(\vec{x'},t',\vec{u},\xi)dt' + e^{-t/\tau}f_0(\vec{x}-\vec{u}t,\vec{u},\xi).$$

$$f_0(\vec{x},\vec{u},\xi)=\begin{cases} f_0^l(\vec{x},\vec{u},\xi), & x<0, \\ f_0^r(\vec{x},\vec{u},\xi), & x>0. \end{cases}$$

$$f_0^{l,r}(\vec{x})=f_{NS}^{l,r}(0,0,0)+\frac{\partial f_{NS}^{l,r}}{\partial x}\Big|_{(0,0,0)}x + \frac{\partial f_{NS}^{l,r}}{\partial y}\Big|_{(0,0,0)}y+\frac{1}{2}\frac{\partial^2 f_{NS}^{l,r}}{\partial x^2}\Big|_{(0,0,0)}x^2 + \frac{1}{2}\frac{\partial^2 f_{NS}^{l,r}}{\partial y^2}\Big|_{(0,0,0)}y^2+\frac{\partial^2 f_{NS}^{l,r}}{\partial x\partial y}\Big|_{(0,0,0)}xy$$

Initial reconstruction:

$W^l(\vec{x})$ & $W^r(\vec{x})$

$\downarrow$ $\downarrow$

f_0^l f_0^r

A high-order NS solver

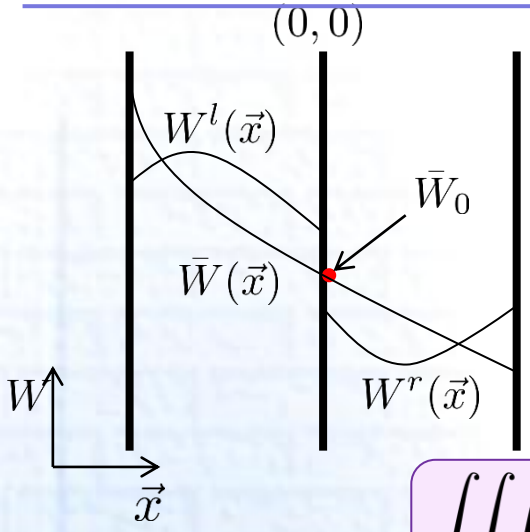

$$g(\vec{x},t) = \bar{g} + \bar{g}_x x + \bar{g}_y y + \bar{g}_t t + \tfrac{1}{2}\bar{g}_{xx}x^2 + \tfrac{1}{2}\bar{g}_{yy}y^2 + \bar{g}_{xy}xy + \tfrac{1}{2}\bar{g}_{tt}t^2 + \bar{g}_{xt}xt + \bar{g}_{yt}yt$$

$$\iiint (g-f)\psi_\alpha \mathrm{d}u\mathrm{d}v\mathrm{d}\xi = 0, \qquad \alpha = 1,2,3,4$$

$$\bar{W}_0 = \iiint \bar{g}\psi \mathrm{d}u\mathrm{d}v\mathrm{d}\xi = \iiint_{u>0} f_0^l(0,0,\vec{u},\xi)\psi \mathrm{d}u\mathrm{d}v\mathrm{d}\xi + \iiint_{u<0} f_0^r(0,0,\vec{u},\xi)\psi \mathrm{d}u\mathrm{d}v\mathrm{d}\xi$$

Equilirium reconstruction from $\bar{W}_0$ and the information of neighboring cells

$\bar{W}(\vec{x})$

$$\iiint [\bar{g}_t(\vec{x},t) + \vec{u}\cdot\nabla\bar{g}(\vec{x},t)]\psi \mathrm{d}u\mathrm{d}v\mathrm{d}\xi = 0$$

$g(\vec{x},t)$

A high-order NS solver

Finite volume scheme in a rectangular cell:

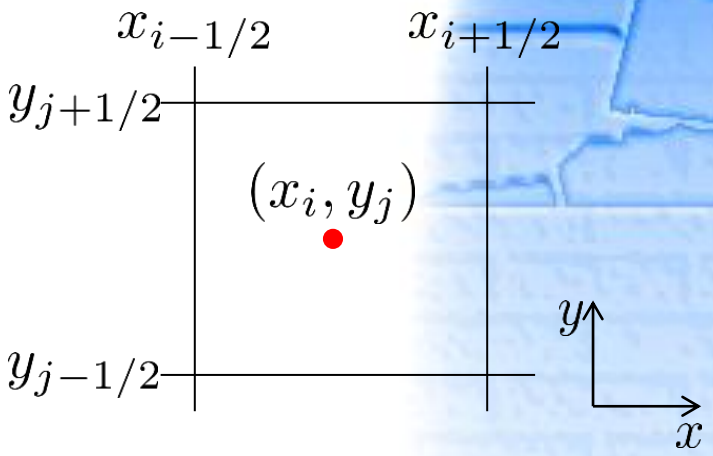

The flux F of the conservative variables at the cell interface:

$$F(\vec{x},t) = \iiint u\psi f(\vec{x},t,\vec{u},\xi)\mathrm{d}u\mathrm{d}v\mathrm{d}\xi$$

$$W_{ij}^{n+1} = W_{ij}^{n} + \frac{1}{\Delta x_i \Delta y_j}\int_{t_n}^{t_{n+1}}\int_{x_{i-1/2}}^{x_{i+1/2}}\left[F_{j-1/2}(t,x) - F_{j+1/2}(t,x)\right]dxdt$$

$$+\frac{1}{\Delta x_i \Delta y_j}\int_{t_n}^{t_{n+1}}\int_{y_{j-1/2}}^{y_{j+1/2}}\left[F_{i-1/2}(t,y) - F_{i+1/2}(t,y)\right]dydt$$

A high-order NS solver

Collision time:

$$f(0,y,t,\vec{u},\xi) = \frac{1}{\tau}\int_0^t g(-ut', y-vt', t', \vec{u}, \xi) e^{-(t-t')/\tau} dt'$$

$$+e^{-t/\tau} f_0(-ut, y-vt, \vec{u}, \xi)$$

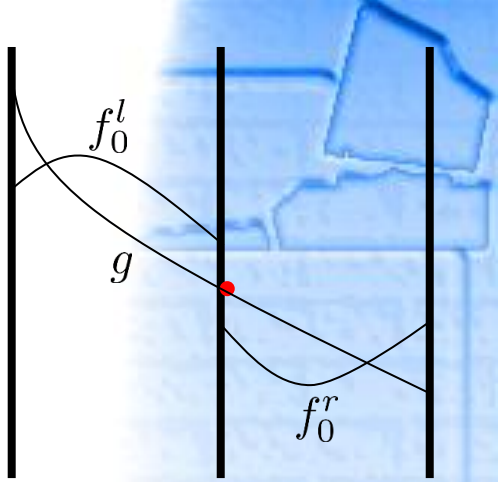

$$f_{NS}(\vec{x},t) = g(\vec{x},t) - \tau[g_t(\vec{x},t) + \vec{u}\cdot\nabla g(\vec{x},t)]$$

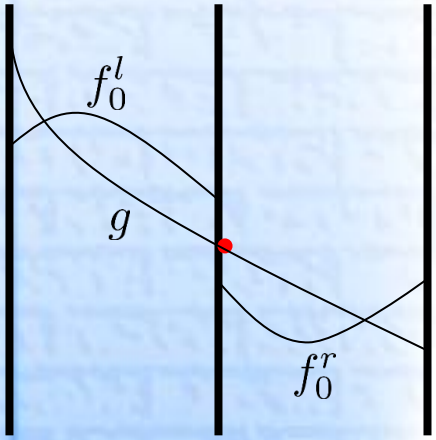

Euler solver:

$$\tau_n = \alpha\Delta x\sqrt{\bar{\lambda}} + \beta\Delta x\sqrt{\bar{\lambda}}|p^l - p^r|/(p^l + p^r)$$

NS solver:

$$\tau = \mu/\bar{p}$$

$$\tau_n = \mu/\bar{p} + \beta\Delta x\sqrt{\bar{\lambda}}|p^l - p^r|/(p^l + p^r)$$

A high-order NS solver

The 5th order WENO reconstruction:

Q : the variable to be reconstructed

$\bar{Q}_i$: the cell averaged value in the ith cell

Q_i^l, Q_i^r : the two pointwise values reconstructed at the left and right interfaces of the ith cell

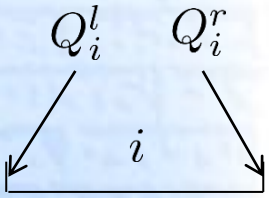

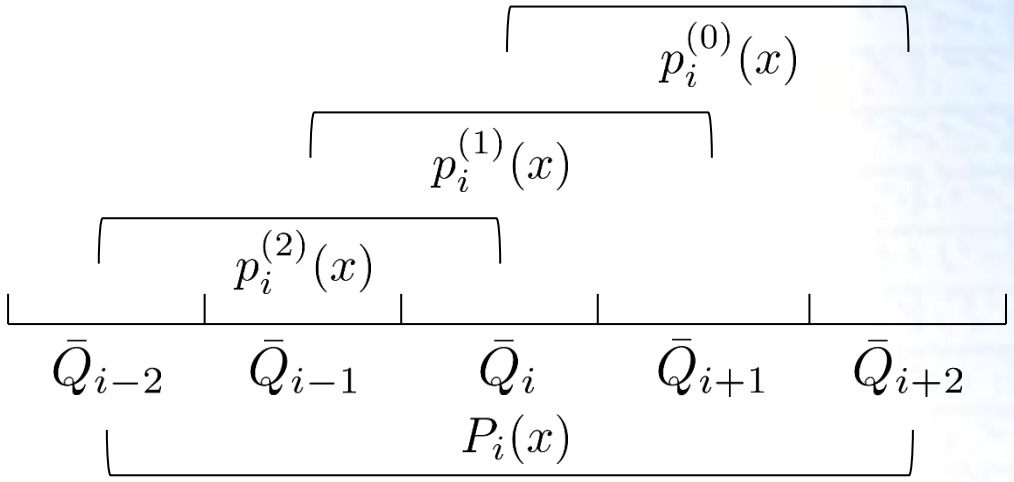

$$P_i(x) = \sum_{l=0}^{2} d_l p_i^{(l)}(x)$$

A high-order NS solver

$$\beta_s = \sum_{l=1}^{2} \int_{x_{i-1/2}}^{x_{i+1/2}} \Delta x^{2l-1} \left(\frac{\partial^l p_i^{(s)}(x)}{\partial x^l} \right) dx$$

$$w_s = \frac{\alpha_s}{\sum_{p=0}^{2} \alpha_p}, \ \alpha_s = \frac{d_s}{(\epsilon + \beta_s)^2}, \ \tilde{w}_s = \frac{\tilde{\alpha}_s}{\sum_{p=0}^{2} \tilde{\alpha}_p}, \ \tilde{\alpha}_s = \frac{\tilde{d}_s}{(\epsilon + \beta_s)^2}, \ s = 0, 1, 2$$

$$q_i^{(s)} = p_i^{(s)}(x_{i+1/2}), \ \tilde{q}_i^{(s)} = p_i^{(s)}(x_{i-1/2}), \ s = 0, \ 1, \ 2$$

$$Q_i^r = \sum_{s=0}^{2} w_s q_i^{(s)}, \ Q_i^l = \sum_{s=0}^{2} \tilde{w}_s \tilde{q}_i^{(s)}$$

In the numerical tests, "EPS1" means $\epsilon = 10^{-6}$ and "EPS2" refers to $\epsilon = 10^{-2}$.

A high-order NS solver

Subcell reconstruction of GKS:

1. The reconstruction of initial subcell flow distributions

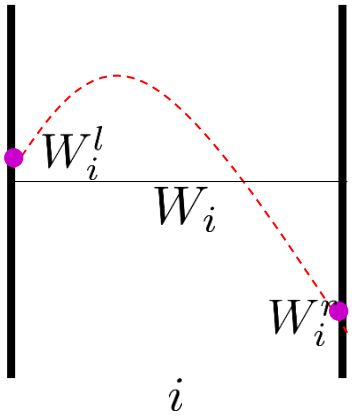

2. The reconstruction of equilibrium high-order derivatives

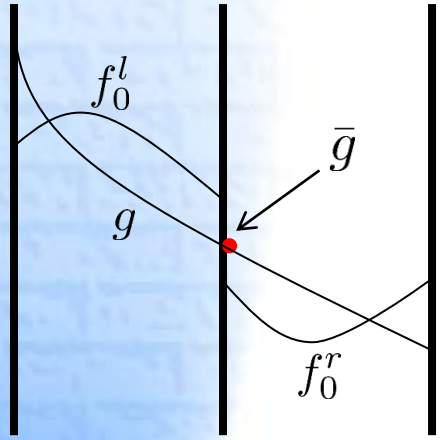

$$\bar{W}_0 = \iiint \bar{g}\psi \mathrm{d}u\mathrm{d}v\mathrm{d}\xi$$

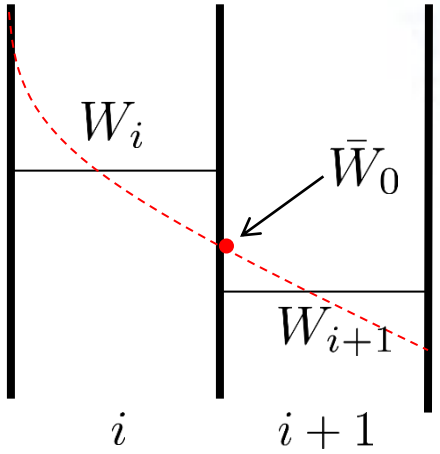

Contents

- PDE-based modeling
- A high-order WENO-gas-kinetic Navier-Stokes flow solver
- The WENO-Steger-Warming scheme
- Numerical results
- Conclusion

WENO-SW scheme

$$W_t + F(W)_x + G(W)_y = F^v(W, W_x, W_y)_x + G^v(W, W_x, W_y)_y$$

F and G : inviscid fluxes
F^v and G^v : viscous fluxes

Steger-Warming splitting:

$$F = F^+ + F^-$$

$$F^\pm = R\Lambda^\pm L,\ \Lambda = \Lambda^+ + \Lambda^-$$

$$\Lambda^\pm = diag[\lambda_1^\pm, \lambda_2^\pm, ..., \lambda_n^\pm] \text{ with } \lambda_i^\pm = \frac{\lambda_i \pm \sqrt{\lambda_i^2 + \varepsilon}}{2} (i = 1, \cdots, n)$$

$\Lambda = diag[\lambda_1, \lambda_2, ..., \lambda_n]$: matrix with diagonal eigenvalues of $\partial F/\partial W$

R/L : right/left eigenvector matrix

WENO-SW scheme

Inviscid flux

The construction of the numerical x-direction flux $\hat{F}_{i+1/2,j}$ at the cell interface $(x_{i+1/2}, y_j)$ of the cell (i, j).

$F_{i+l,j}(l = -2, \cdots, 3)$ —the Steger-Warming splitting→ $F^{\pm}_{i+l,j}(l = -2, \cdots, 3)$

$W_{i+1/2,j} = (W_{i,j} + W_{i+1,j})/2$ → $L_{i+1/2,j}$ and $R_{i+1/2,j}$

Characteristic fluxes:
$\tilde{F}^{\pm}_{i+l,j} = L_{i+l/2,j} F^{\pm}_{i+l,j} \quad (l = -2, \cdots, 3)$ —WENO reconstruction→ $\tilde{F}^{\pm}_{i+1/2,j}$

$\tilde{F}_{i+1/2,j} = \tilde{F}^{+}_{i+1/2,j} + \tilde{F}^{-}_{i+1/2,j}$ → $\hat{F}_{i+1/2,j} = R_{i+1/2,j} \tilde{F}_{i+1/2,j}$

WENO-SW scheme

Viscous flux

In each cell (i, j),

$$\left(\frac{\partial q}{\partial x}\right)_{i,j} = \frac{45(q_{i+1,j} + q_{i-1,j}) - 9(q_{i+2,j} - q_{i-2,j}) + q_{i+3,j} - q_{i-3,j}}{60\Delta x},$$

where q could be T, U or V.

$$F^v_{i,j}$$

$$\hat{F}^v_{i+1/2,j} = \frac{37(F^v_{i,j} + F^v_{i+1,j}) - 8(F^v_{i-1,j} + F^v_{i+2,j}) + F^v_{i-2,j} + F^v_{i+3,j}}{60}$$

Contents

- PDE-based modeling
- A high-order WENO-gas-kinetic Navier-Stokes flow solver
- The WENO-Steger-Warming scheme
- Numerical results
- Conclusion

Mach 3 step problem:

Computational domain: $[0, 3] \times [0, 1]$ BC: adiabatic slip Euler BC
Step location: $x = 0.55$ Step height: 0.2 Upstream velocity: $(U, V) = (3, 0)$

WENO-GSK-Euler

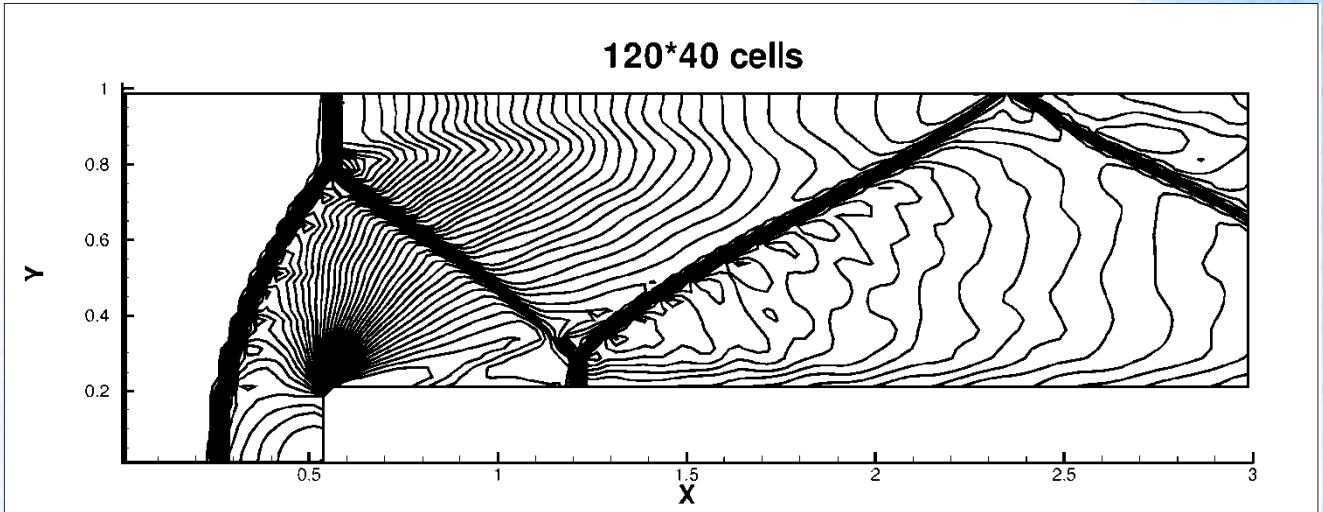

WENO-SW

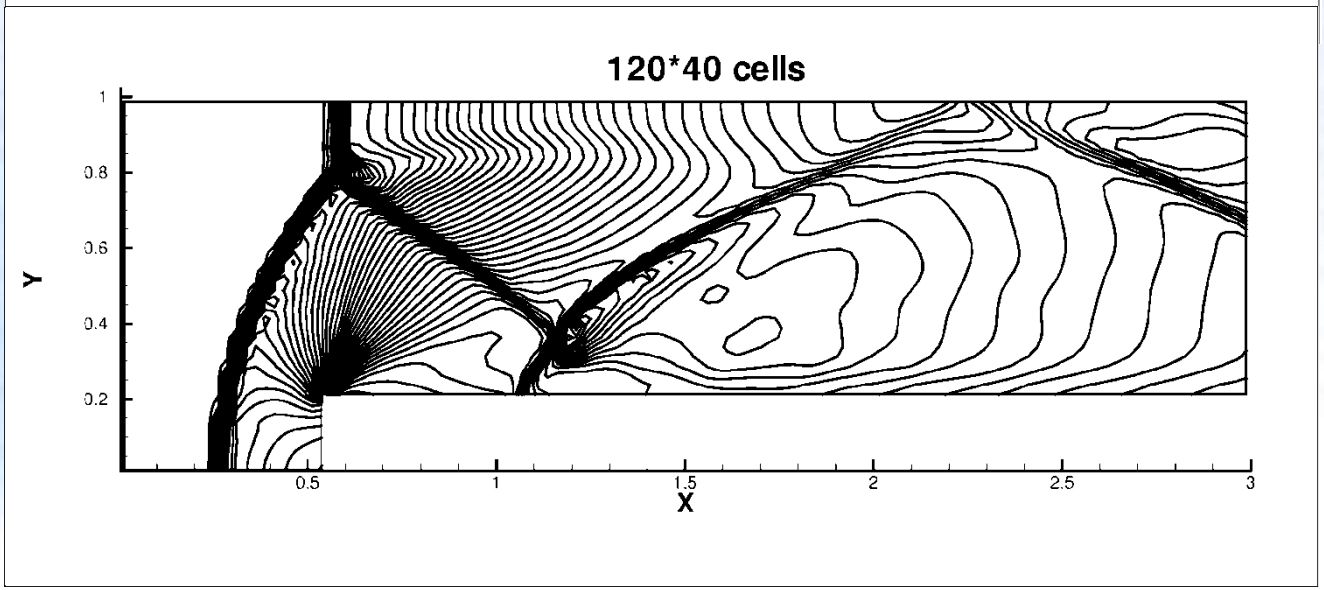

Numerical results

WENO-GSK-Euler

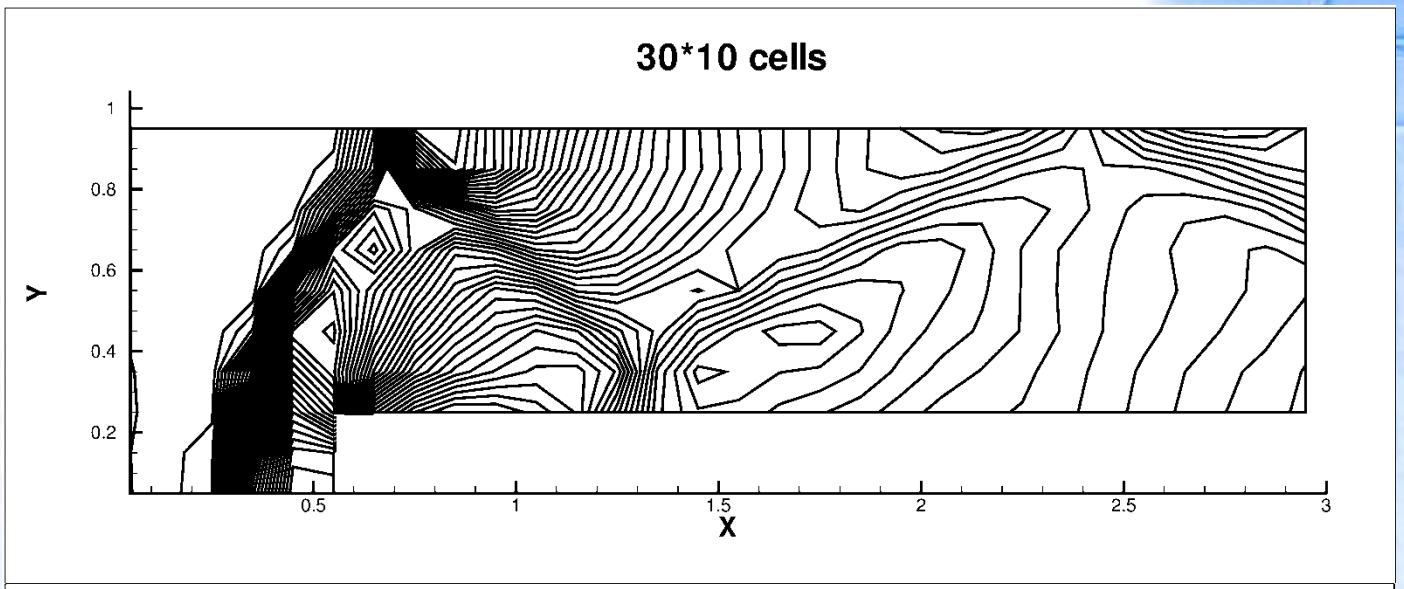

WENO-SW

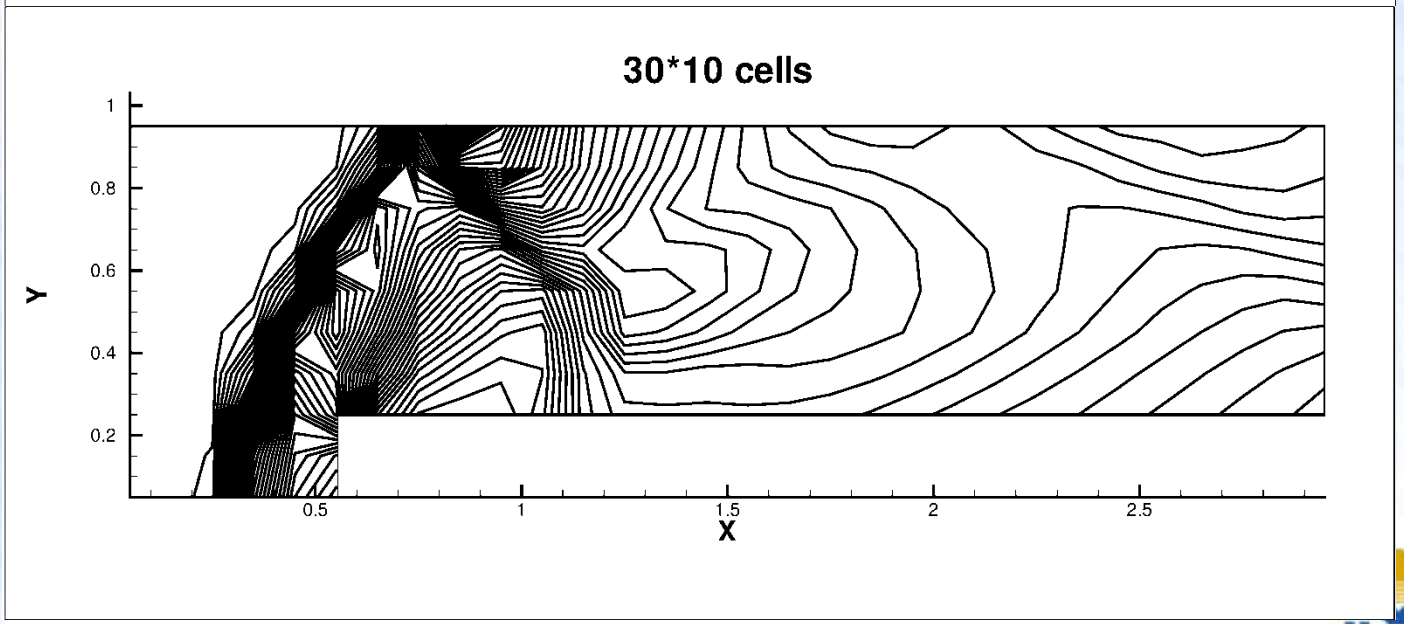

Isentropic periodic vortex propagation:

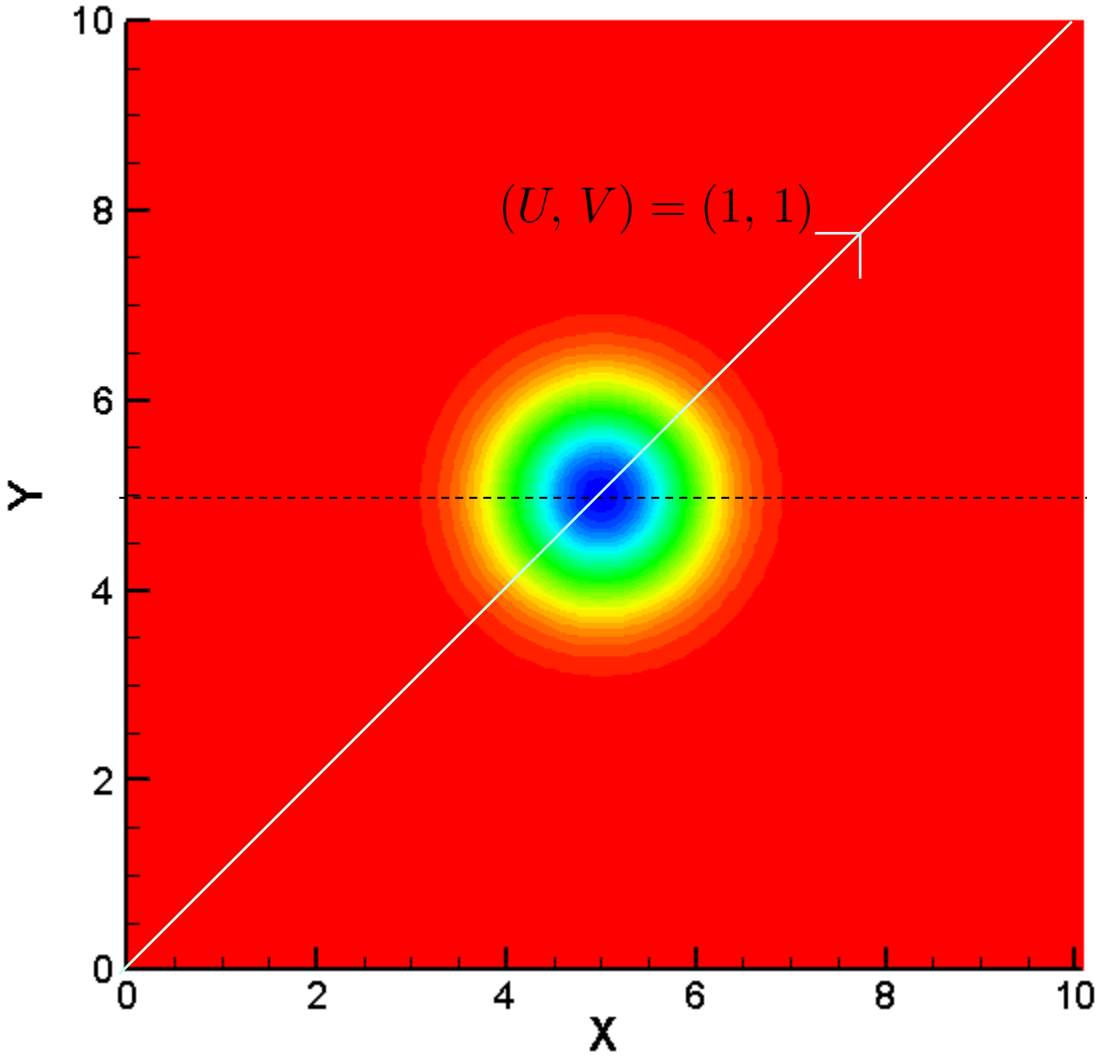

Numerical results

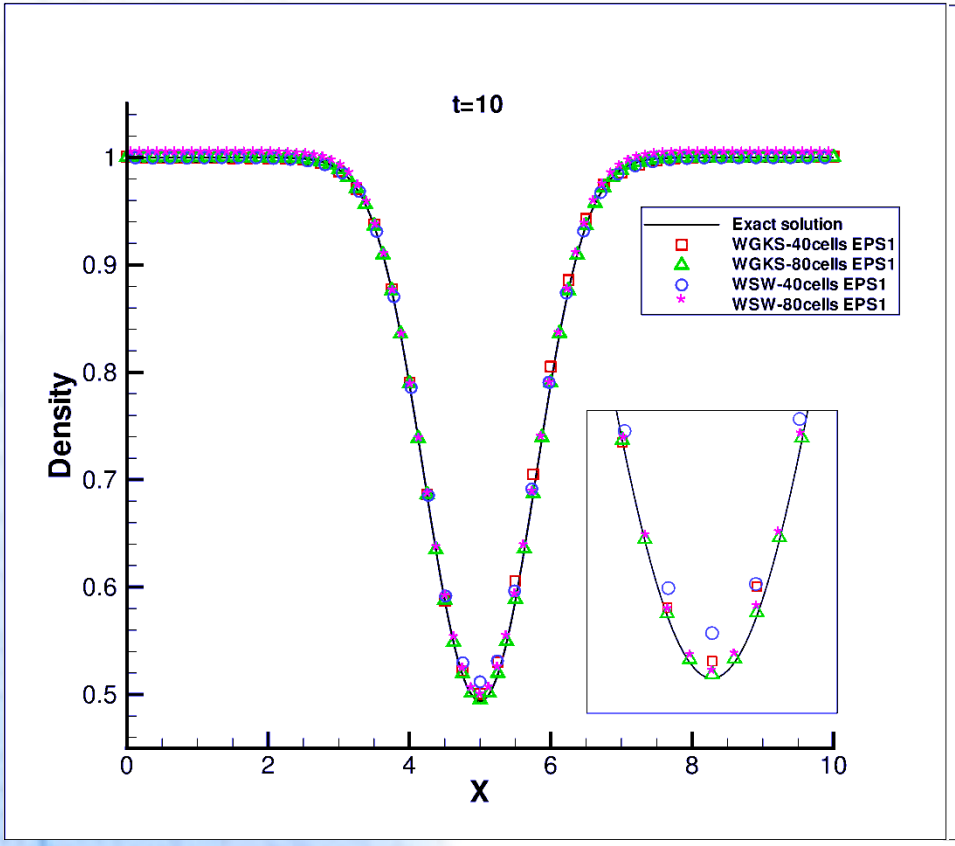

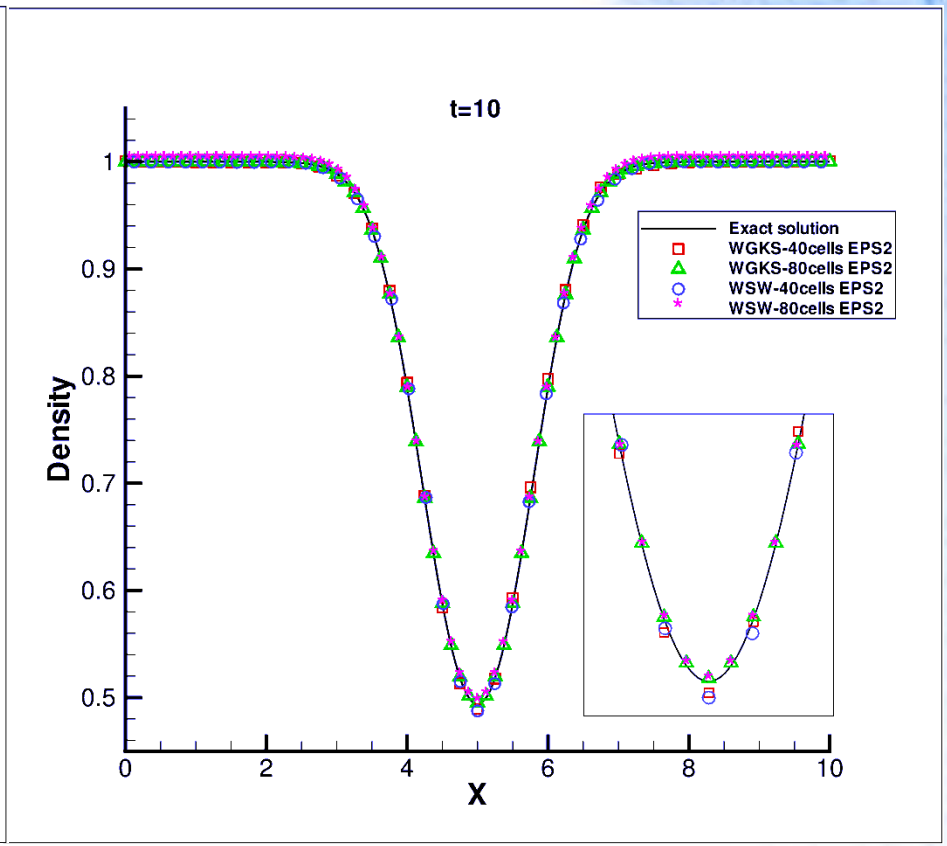

Numerical results

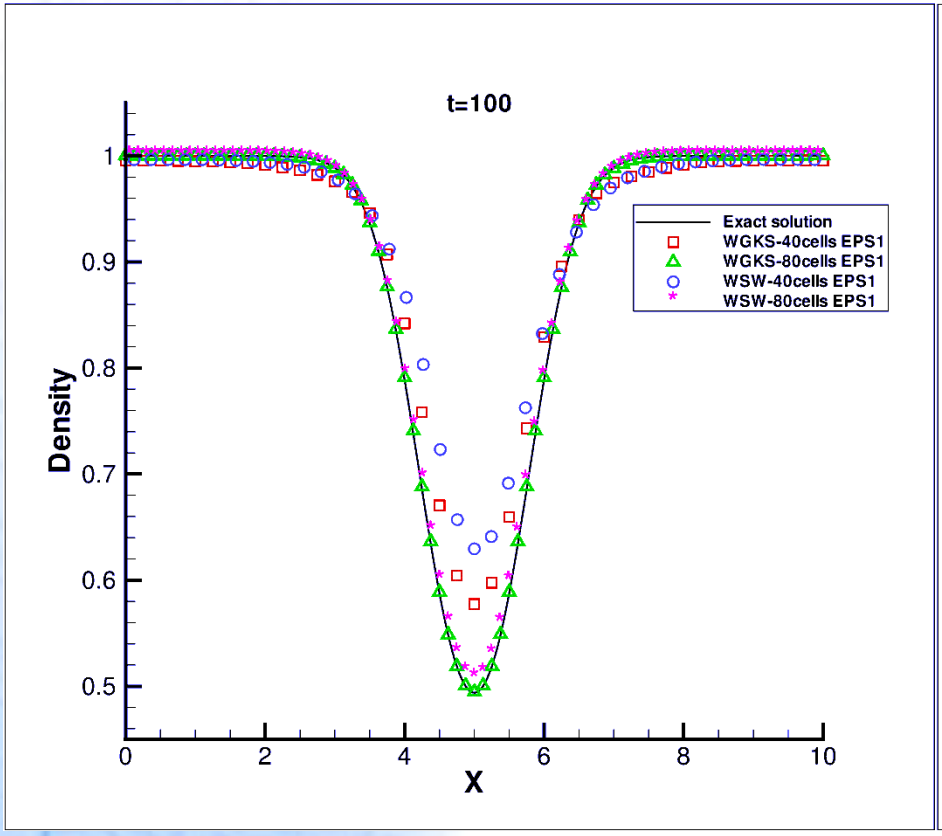

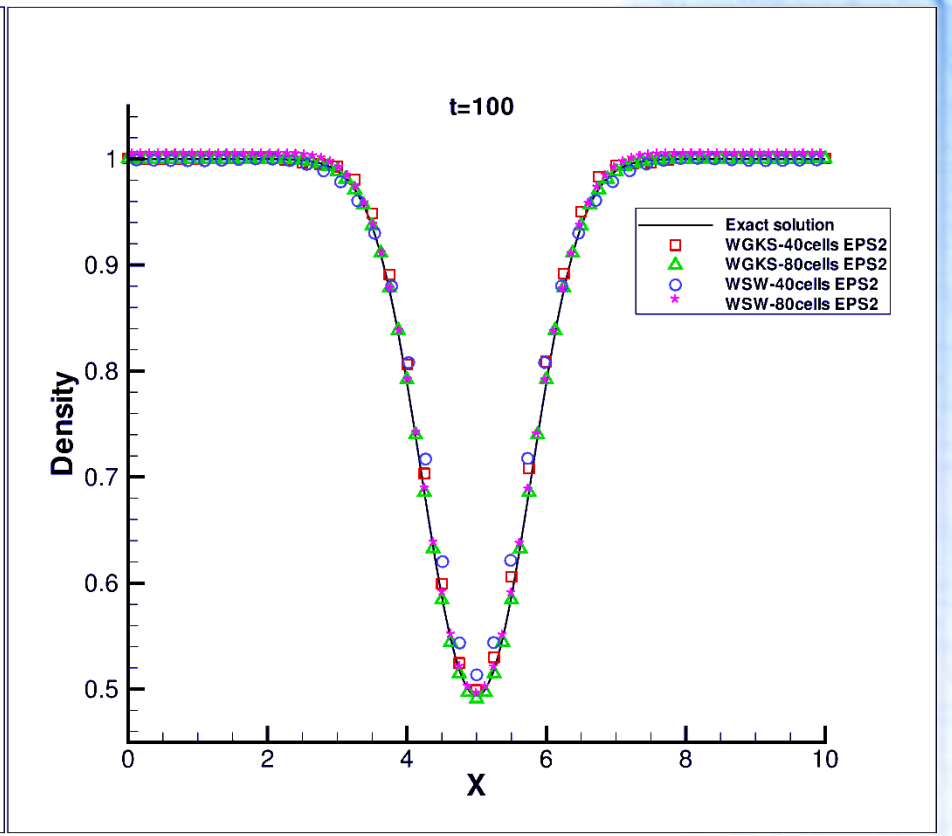

Cavity flow:

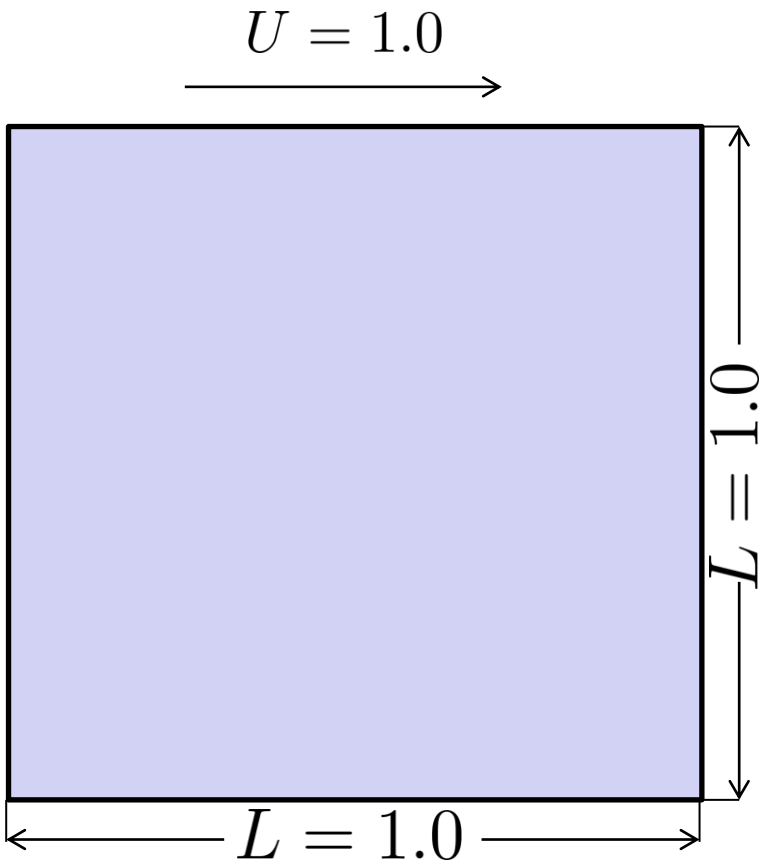

$Mach = 0.3,\ Re = 3200$

Numerical results

$Re = 3200$, 65 cells

WENO-GKS-NS

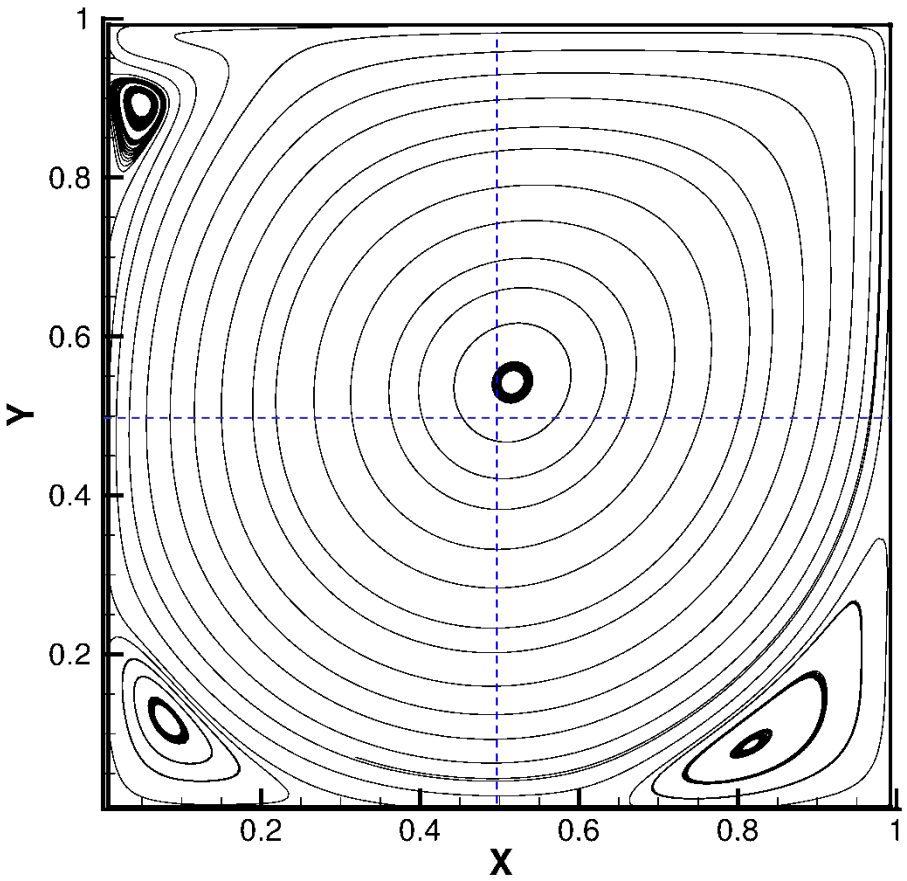

WENO-SW

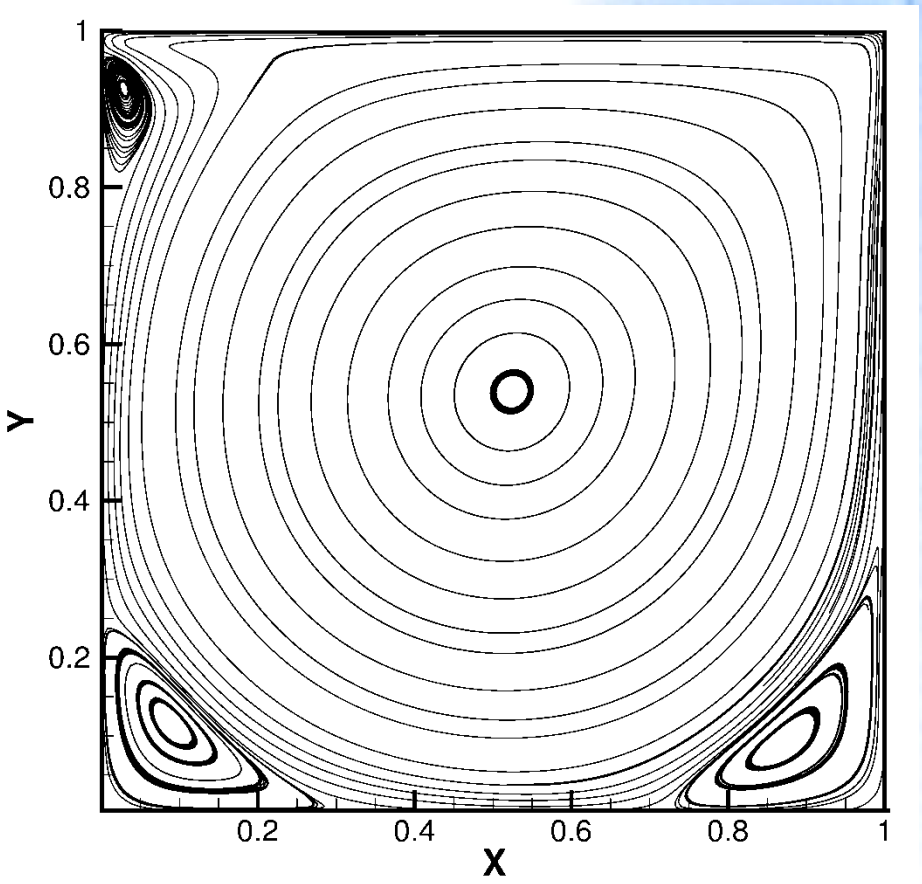

Numerical results

$Re = 3200$, 65 cells

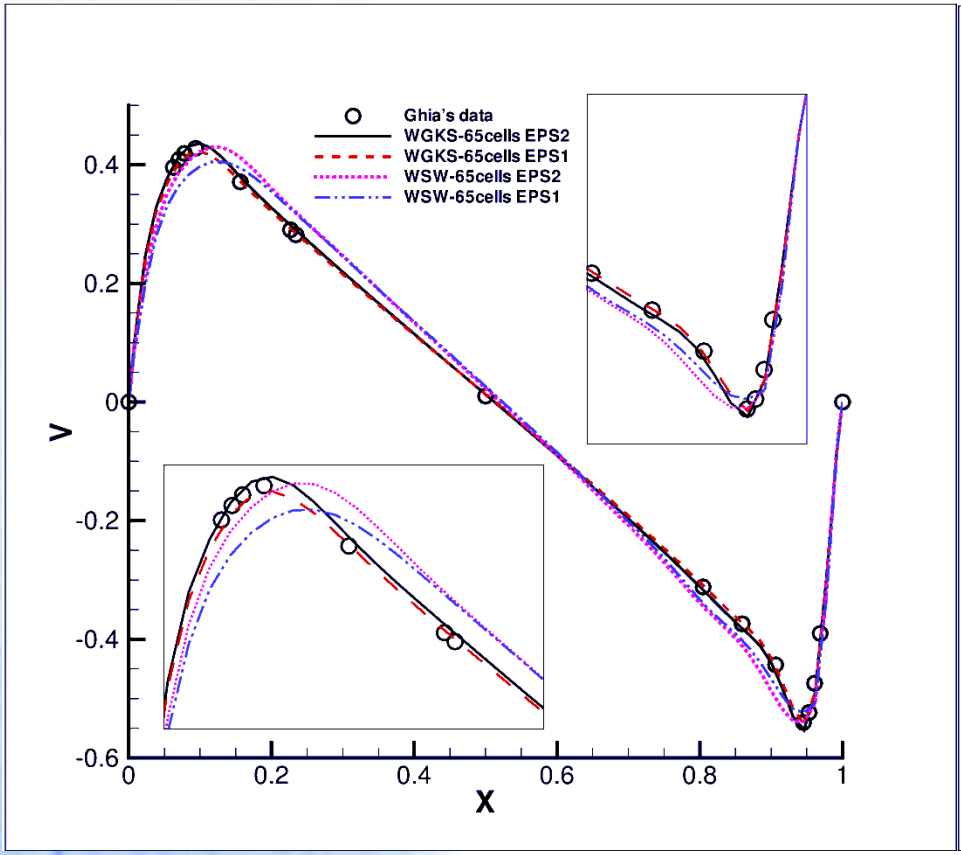

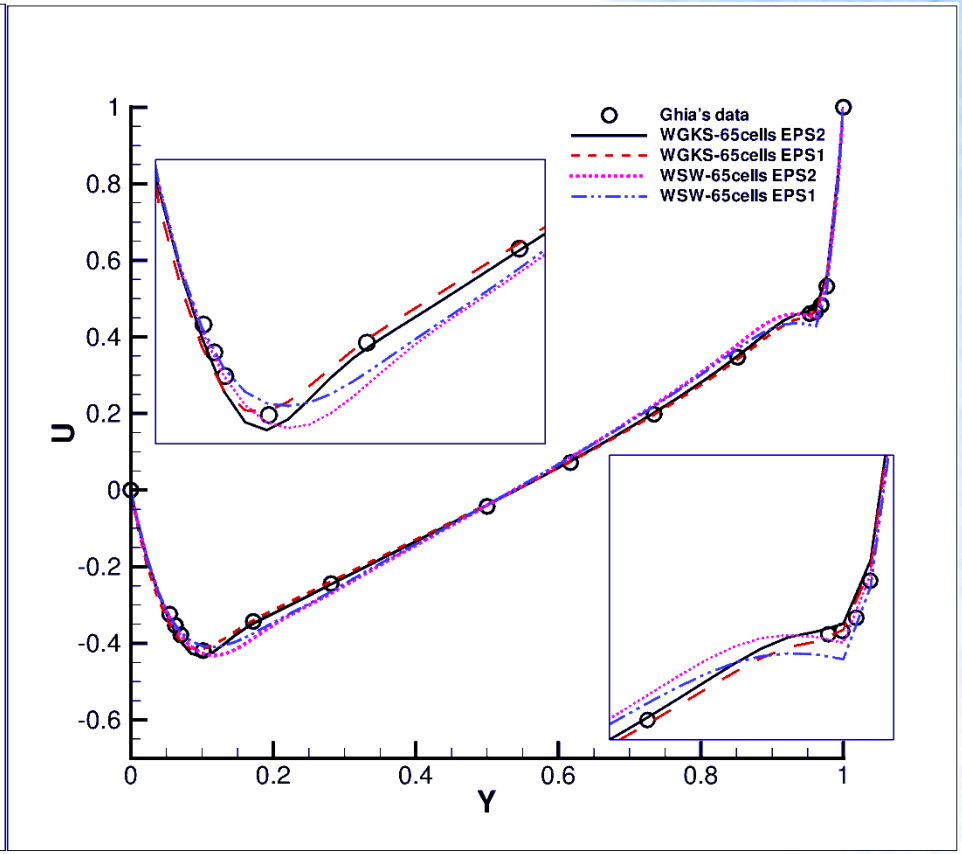

Numerical results

$Re = 3200$, 33 cells

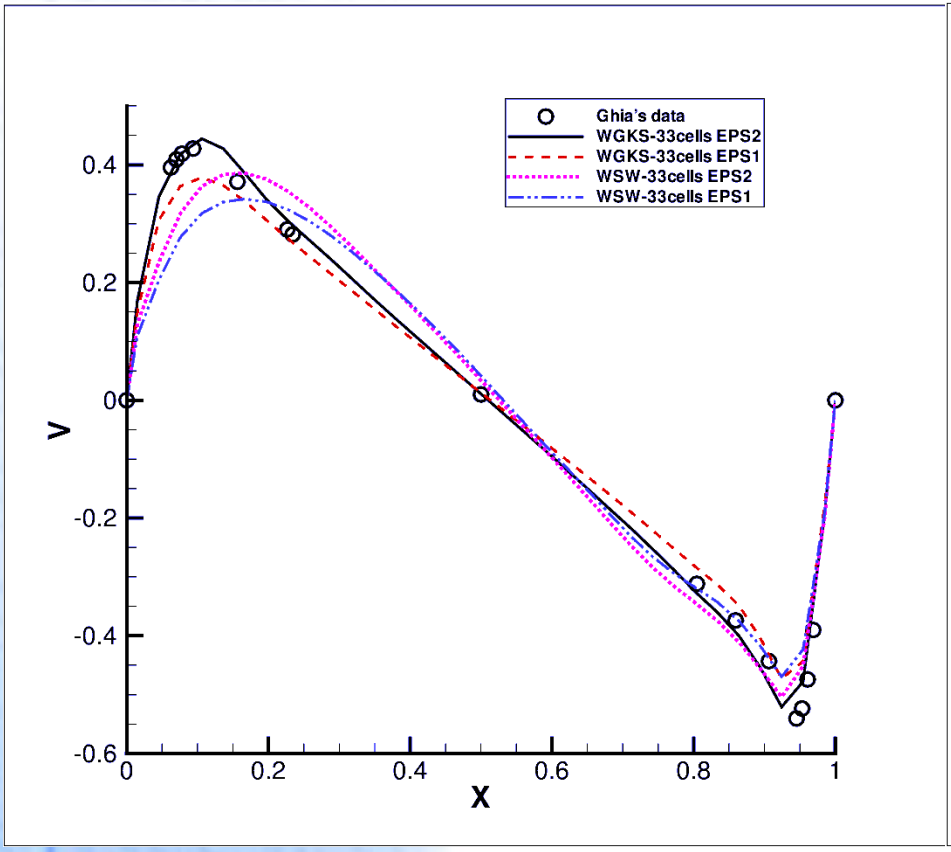

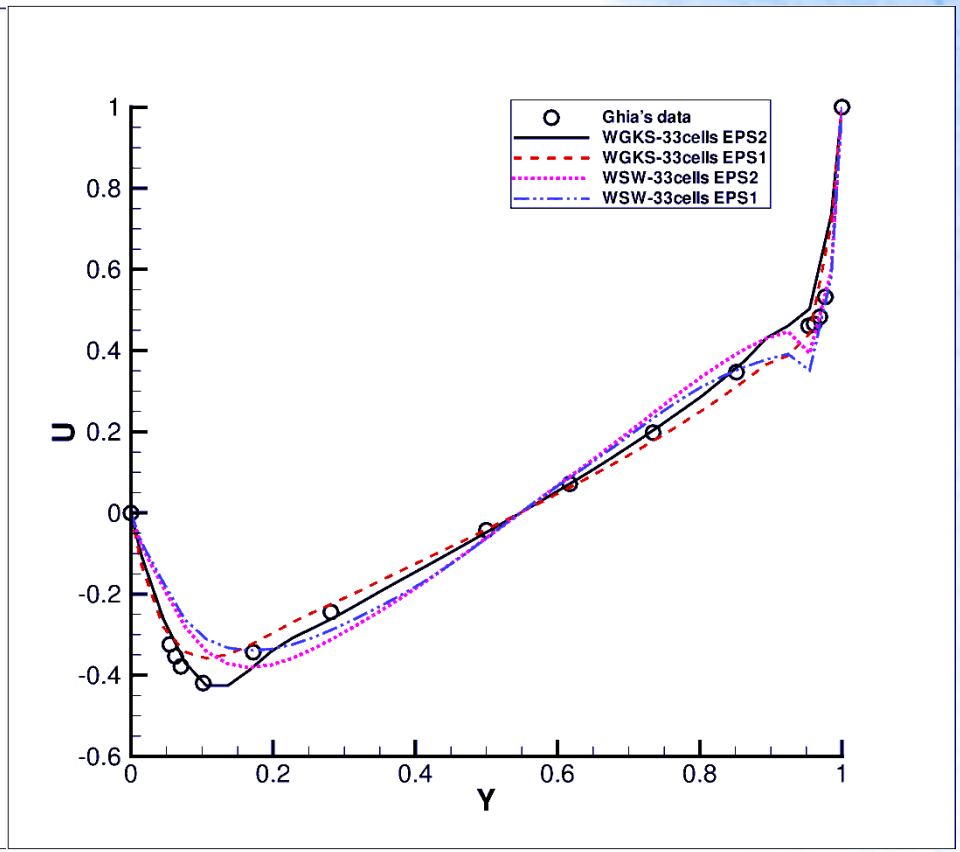

Numerical results

$$\text{Error}(t) = \frac{\sum_{i,j} |\rho(x_i,y_j,t) - \rho(x_i,y_j,t-10)|}{\mathcal{N}}$$

$\mathcal{N}$: number of cells

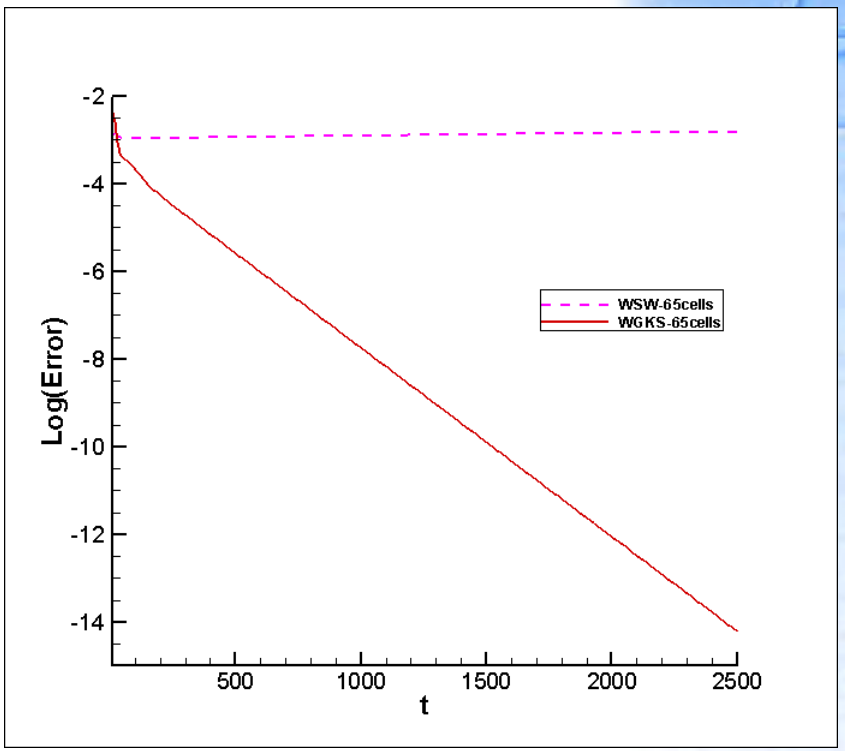

Computational time

Average computational time for one time-step in cavity flow simulation:

CPU time(seconds)	WENO-GKS	WENO-SW
$33 \times 33\, cells$	1.8776e-002	4.3276e-003
$65 \times 65\, cells$	7.4369e-002	1.6433e-002

Contents

- PDE-based modeling
- A high-order WENO-gas-kinetic Navier-Stokes flow solver
- The WENO-Steger-Warming scheme
- Numerical results
- Conclusion

Conclusion

- Both WENO-SW and WENO-GKS yield quantitatively similar results when a sufficient mesh points are used to resolve the flow structure. With the reduction of mesh points, the WENO-GKS appears to have less numerical dissipation than the WENO-SW.
- Due to the operator splitting approach to discretize the inviscid and viscous terms, in the cavity flow simulation, the solution of the WENO-SW is more sensitive to the boundary treatment or the reconstruction scheme.
- Because of its smooth transition from the upwind to the central difference flux construction, the WENO-GKS is not sensitive to the initial discontinuous point-wise data reconstruction at the cell interface.

  Besides high-order initial reconstruction, a reliable gas evolution model is important in the construction of high-order schemes.

Thank you